

$\bar{p}p$ -annihilation processes in the tree approximation of SU(3) chiral effective theory

V.E. Tarasov¹, A.E. Kudryavtsev¹, A.I. Romanov^{1,2}, V.M. Weinberg^{1,3}

¹*Institute of Theoretical and Experimental Physics, Moscow, 117218, Russia*

²*National Research Nuclear University MEPhI, Moscow, 115409, Russia*

³*Moscow Institute of Physics and Technology, Moscow district, 141700, Russia*

The $\bar{p}p$ -annihilation reactions $\bar{p}p \rightarrow \eta\eta\eta$ and $\bar{p}p \rightarrow \eta K \bar{K}$ at rest are considered in the tree approximation in the framework of SU(3) chiral effective theory at leading order. The calculated branchings are compared with the data. The results for neutral ($\eta\eta\eta$, $K^0 \bar{K}^0 \eta$) and charged ($K^+ K^- \eta$) channels are essentially different.

Pacs numbers: 12.39.Fe, 13.60.Le, 13.75.Cs, 25.43.+t.

1 Introduction

Nowadays, the QCD formulated in terms of quark and gluon fields is confirmed as the fundamental theory of strong interactions. However, the quantitative predictions for hadronic reactions meet with unsolved problems coming from a non-perturbative character of the QCD at large distances. The alternative effective field approach, successfully applied in the low-energy hadron physics, is the so-called Chiral Perturbation Theory (ChPT). This theory is based on the internal $SU(3)_L \times SU(3)_R \times U(1)_V$ symmetry of QCD, violated by quark masses, and is formulated in terms of hadrons – mesons (as the Goldstone bosons) and baryons. The ChPT, more than 30-year history of which can be traced back to the pioneering works by Weinberg [1] and Gasser and Leutwyler [2], has developed into a powerful tool for investigating the $\pi\pi$ [3], πN [4, 5] as well as the few nucleon systems [6, 7]. A large number of references can be found in the reviews [8–11]. The Lagrangian of the effective theory may generally contain infinite number of terms with different number of derivatives and unknown constants, and ChPT makes sense only at small particle momenta (p) and meson masses (μ), i.e., at $p, \mu \ll \Lambda_\chi = 4\pi f_\pi \sim 1 \text{ GeV}$, where $f \approx 93 \text{ MeV}$ is the pion decay constant. In this case we have the expansion parameter $\chi \sim \mu/\Lambda_\chi \ll 1$, and the leading-order (LO) term of the Lagrangian is well defined.

In this paper we make the first attempt to apply the ChPT to the annihilation processes $N\bar{N} \rightarrow$ mesons. We are interested in the case of slow final mesons (with momenta $k \ll \Lambda_\chi$) in the reaction rest frame. This situation takes place, for example, in the multi-pion annihilation process $N\bar{N} \rightarrow n\pi$ with large $n \sim \sqrt{s}/\mu \gg 1$. The appropriate data up to $n = 9$, obtained from $p\bar{p}$ annihilation at rest can be found in [12]. Theoretical study of such

processes involves calculation of a large number of diagrams and integration over the final many-particle phase space. In this respect, the reactions with a small number of heavier final mesons η and $K(\bar{K})$ seem to be more attractive, and corresponding data are available as well [13]. In this paper, we consider the $p\bar{p}$ annihilation processes

$$(a) \bar{p}p \rightarrow \eta\eta\eta, \quad (b) \bar{p}p \rightarrow \eta K^0 \bar{K}^0, \quad (c) \bar{p}p \rightarrow \eta K^+ K^- \quad (1)$$

at rest. Here, the typical meson momentum is $k \sim 300 \text{ MeV}/c$, the ChPT expansion parameter value $\chi \sim \mu/\Lambda_\chi \sim 0.5$, and we may expect a sensible results from LO calculations in the effective chiral theory. In the present paper, we perform calculations for the probabilities (branchings) of the reactions (1) at rest in the tree approximation, using the SU(3) chiral effective Lagrangian at LO [9, 10].

The paper is organized as follows. In Section 2, we describe the $SU(3)$ chiral Lagrangian and write down its parts used in the tree calculations. In Section 3, we calculate the amplitudes for the reactions (1). In Section 4, we present our numerical results for the branchings, compare them with the experiment and discuss the results. Section 5 is the Conclusion.

2 Lagrangian

We consider the $SU(3)$ chiral effective Lagrangian at leading order. The meson part $\mathcal{L}_{\pi\pi}$ of the Lagrangian can be written in the form

$$\mathcal{L}_{\pi\pi} = \mathcal{L}_1 + \mathcal{L}_2, \quad (2)$$

$$\mathcal{L}_1 = \frac{f^2}{4} \langle \partial_\mu U \partial^\mu U^\dagger \rangle, \quad \mathcal{L}_2 = \sigma \frac{f^2}{2} \langle U M^\dagger + M U^\dagger \rangle, \quad U = \exp\left(\frac{2i\pi}{f}\right),$$

$$\pi = \frac{1}{2} \sum \pi_a(x) \lambda_a = \frac{1}{\sqrt{2}} \begin{pmatrix} \frac{1}{\sqrt{2}} \pi^0 + \frac{1}{\sqrt{6}} \eta & & \pi^+ & K^+ \\ \pi^- & -\frac{1}{\sqrt{2}} \pi^0 + \frac{1}{\sqrt{6}} \eta & & K^0 \\ K^- & & \bar{K}^0 & -\frac{2}{\sqrt{6}} \eta \end{pmatrix}.$$

Here, π is the octet matrix of the meson fields, and U represents their customary exponential parametrization; λ_a ($a = 1, \dots, 8$) are the Gell-Mann matrices, normalized as $\langle \lambda_a \lambda_b \rangle = 2\delta_{ab}$; the angle brackets $\langle \dots \rangle$ denote the trace over flavours; $f \approx 93 \text{ MeV}$ is the pion decay constant; $M = \text{diag}(m_u, m_d, m_s)$ is the quark-mass matrix. The first term \mathcal{L}_1 in Eq. (2) is the chiral symmetrical part of the Lagrangian $\mathcal{L}_{\pi\pi}$. The second term \mathcal{L}_2 contains the quark-mass matrix M and spontaneously violates the chiral symmetry. The parameter σ in the term \mathcal{L}_2 relates the meson and quark masses in the form

$$\begin{aligned} m_\pi^2 &= \sigma(m_u + m_d), & m_{K^\pm}^2 &= \sigma(m_u + m_s), \\ m_{K^0, \bar{K}^0}^2 &= \sigma(m_d + m_s), & m_\eta^2 &= \frac{1}{3}\sigma(m_u + m_d + 4m_s), \end{aligned} \quad (3)$$

known as the Gell-Mann, Oakes and Renner relations [14].⁴⁾ To obtain Eqs. (3) one can expand the Lagrangian \mathcal{L}_2 (2) in the meson fields and identify the quadratic term for a given meson π_a with the mass term $-\frac{1}{2}m^2\pi_a^2$.

The baryon-meson part of the effective Lagrangian can be written as

$$\mathcal{L}_{\pi B} = \mathcal{L}_3 + \mathcal{L}_4, \quad (4)$$

$$\mathcal{L}_3 = \langle \bar{B}(i\mathcal{D}_\mu\gamma^\mu - m_B)B \rangle, \quad \mathcal{L}_4 = \langle \bar{B}\gamma^\mu\gamma_5(D\{A_\mu, B\} + F[A_\mu, B]) \rangle.$$

where

$$\begin{aligned} \mathcal{D}_\mu &= \partial_\mu B + [V_\mu, B], & V_\mu &= \frac{1}{2}(\xi\partial_\mu\xi^+ + \xi^+\partial_\mu\xi), \\ A_\mu &= \frac{i}{2}(\xi\partial_\mu\xi^+ - \xi^+\partial_\mu\xi), & \xi &= \exp\left(\frac{i\pi}{f}\right) = \sqrt{U}, \end{aligned} \quad (5)$$

$$B = \frac{1}{\sqrt{2}} \sum B_a(x)\lambda_a = \begin{pmatrix} \frac{1}{\sqrt{2}}\Sigma^0 + \frac{1}{\sqrt{6}}\Lambda & & \Sigma^+ & & p \\ & \Sigma^- & & -\frac{1}{\sqrt{2}}\Sigma^0 + \frac{1}{\sqrt{6}}\Lambda & n \\ & & \Xi^- & & \Xi^0 \\ & & & & -\frac{2}{\sqrt{6}}\Lambda \end{pmatrix}.$$

Here, B is the octet matrix of the baryon fields; m_B is the baryon mass; D and F are the usual axial-vector meson-baryon coupling constants; $[A, B]$ and $\{A, B\}$ mean commutator and anticommutator for the operators A and B .

We expand the Lagrangians $\mathcal{L}_{\pi\pi}$ (2) and $\mathcal{L}_{\pi B}$ (4) in meson fields and retain only the interaction terms of interest for the $\bar{p}p \rightarrow (3 \text{ mesons})$ amplitude in the tree approximation. So, we use the terms of the fourth order in meson fields from $\mathcal{L}_{\pi\pi}$ and the terms up to the third order from $\mathcal{L}_{\pi B}$. Then, the total interaction Lagrangian takes the form

$$L = L_1 + L_2 + L_3 + L_4, \quad (6)$$

$$\begin{aligned} L_1 &= \frac{1}{3f^2} \langle [\partial^\mu\pi, \pi][\partial_\mu\pi, \pi] \rangle, & L_2 &= \frac{2\sigma}{3f^2} \langle M\pi^4 \rangle, \\ L_3 &= i \langle \bar{B}\gamma^\mu[V_\mu, B] \rangle, & L_4 &= \mathcal{L}_4 \text{ (see Eq. (4))}, \\ V_\mu &= \frac{1}{2f^2} [\pi, \partial_\mu\pi], & A_\mu &= \frac{1}{f} \partial_\mu\pi - \frac{1}{6f^3} [[\partial_\mu\pi, \pi], \pi], \end{aligned}$$

Finally, since $m_{u,d} \ll m_s$, we take the u and d quarks to be massless. Thus, we have $M = \text{diag}(0, 0, m_s)$ and $\sigma = 3m_\eta^2/4m_s$ (see Eqs. (3)) for the term L_2 in Eqs. (6).

⁴⁾These also include the equation for the quark condensate $\langle q\bar{q} \rangle = -3\sigma f^2$.

3 The amplitudes

The full sets of the tree diagrams for the reactions (1a) and (1b), (1c) are shown in Figs. 1 and 2, respectively. Here we write down the corresponding amplitudes. The vertices of these diagrams with a given mesons and baryons are fixed by the Lagrangians L_{1-4} , and are given in Section 1 of Appendix. We shall use the notations:

$$\not{k} \equiv k^\mu \gamma_\mu, \quad G_B(p) = \frac{\not{p} + m_B}{p^2 - m_B^2 + i0}, \quad u = \sqrt{2m} \begin{pmatrix} \varphi \\ 0 \end{pmatrix}, \quad \bar{v} = \sqrt{2m} (0, -\chi^+). \quad (7)$$

Hereafter, $G_B(p)$ is the propagator of baryon with 4-momentum p ; $u(\bar{v})$ is the bispinor of the initial proton(antiproton) at rest; φ and χ are the spinors ($\varphi^+ \varphi = \chi^+ \chi = 1$); m is the proton mass.

3.1. The reaction $\bar{p}p \rightarrow \eta\eta\eta$

The amplitudes for the reaction (1a) read

$$\begin{aligned} iM_A &= V_{p\bar{p}\eta}^3 \bar{v} \not{k}_3 \gamma_5 G_p(k_3 - p_2) \not{k}_2 \gamma_5 G_p(p_1 - k_1) \not{k}_1 \gamma_5 u + (k_1 k_2 k_3 \text{ permutations}), \\ iM_B &= V_{p\bar{p}\eta} V_{\eta^4}^{(2)} X G_\eta, \quad X = \bar{v} \not{P} \gamma_5 u = -4m^2 (\chi^+ \varphi). \end{aligned} \quad (8)$$

Here, $k_i = (\omega_i, \mathbf{k}_i)$ are the 4-momenta of the final η mesons; $p_1(p_2) = (m, \vec{0})$ is the 4-momentum of the initial proton(antiproton) at rest, and $P = p_1 + p_2$ is the total 4-momentum; $G_p(\dots)$ is the proton propagator ($B=p$, see Eq.(7)); $G_\eta = 1/(4m^2 - m_\eta^2)$ is the η propagator in the diagram (B); $V_{p\bar{p}\eta}$ and $V_{\eta^4}^{(2)}$ are the vertex constants, given in Section 1 of Appendix. The amplitude M_A (8) contains $3! = 6$ terms, arising from permutations of η 's momenta k_i .

Further, we express the amplitudes M (8) in the form

$$iM = \chi^+ (A + i\boldsymbol{\sigma}\mathbf{B}) \varphi, \quad (9)$$

making use of Eqs. (7). Then for the diagrams in Fig. 1 we obtain

$$\begin{aligned} (A): \quad A, \mathbf{B} &= (\text{see Section 2 of Appendix}); \\ (B): \quad A &= -4m^2 V_{p\bar{p}\eta} V_{\eta^4}^{(2)} G_\eta, \quad \mathbf{B} = 0. \end{aligned} \quad (10)$$

We also consider the simplified amplitudes, calculated with final mesons at rest. In this "threshold" s -wave approximation we take

$$\mathbf{k}_i = 0, \quad \omega_i = \mu_i + \frac{T}{3}, \quad T = 2m - \mu_1 - \mu_2 - \mu_3, \quad (11)$$

where μ_i are the meson masses, and T is the total kinetic energy (the final mesons are produced at rest as if their masses are $\bar{\mu}_i = \omega_i$). In this case we have two graphs

$$(A): \quad A^{(0)} = \frac{3! V_{p\bar{p}\eta}^3 2m\omega_\eta^3}{(2m - \omega_\eta)^2}, \quad (B): \quad A^{(0)} = A(\text{Eq. (10)}). \quad (12)$$

and the terms of the type $i\sigma\mathbf{B}$ vanish (we use a superscript “(0)” for the amplitudes in the “threshold” approximation).

3.2. The reactions $\bar{p}p \rightarrow \eta K \bar{K}$

The diagrams for these reactions are shown in Fig. 2. Let us denote here the 4-momenta of final η , K and \bar{K} by k_1 , k_2 and k_3 , respectively. Making use of the Lagrangians, given in Section 1 of Appendix, we obtain the $\bar{p}p \rightarrow \eta K \bar{K}$ amplitudes in the form

$$\begin{aligned} iM_{A_1} &= V_{p\bar{p}\eta} V_{p\bar{A}K}^2 \bar{v} \not{k}_3 \gamma_5 G_A(k_3 - p_2) \not{k}_2 \gamma_5 G_p(p_1 - k_1) \not{k}_1 \gamma_5 u, \\ iM_{A_2} &= V_{p\bar{p}\eta} V_{p\bar{A}K}^2 \bar{v} \not{k}_1 \gamma_5 G_p(k_1 - p_2) \not{k}_3 \gamma_5 G_A(p_1 - k_2) \not{k}_2 \gamma_5 u, \\ iM_{A_3} &= V_{A\bar{A}\eta} V_{p\bar{A}K}^2 \bar{v} \not{k}_3 \gamma_5 G_A(k_3 - p_2) \not{k}_1 \gamma_5 G_A(p_1 - k_2) \not{k}_2 \gamma_5 u; \end{aligned} \quad (13)$$

$$\begin{aligned} iM_B(1, a) &= 2V_{1a} (2m\omega_\eta + m_K^2 - m_{K\bar{K}}^2) X G_a, \\ iM_B(2, a) &= V_{2a} X G_a, \quad (a = \eta, \pi^0), \quad V_{ia} = V_{p\bar{p}a} V_{a\eta K \bar{K}}^{(i=1,2)}; \end{aligned} \quad (14)$$

$$iM_C = -V_C \bar{v} (2\not{k}_1 - \not{k}_2 - \not{k}_3) \gamma_5 u, \quad V_C = V_{p\bar{p}\eta K \bar{K}}; \quad (15)$$

$$\begin{aligned} iM_{D_1} &= -V_D \bar{v} \not{k}_3 \gamma_5 G_A(k_3 - p_2) (\not{k}_2 - \not{k}_1) u, \\ iM_{D_2} &= -V_D \bar{v} (\not{k}_1 - \not{k}_3) G_A(p_1 - k_2) \not{k}_2 \gamma_5 u, \quad V_D = V_{p\bar{A}K} V_{p\bar{A}K\eta} \\ iM_{F_1} &= -V_F \bar{v} \not{k}_1 \gamma_5 G_A(k_1 - p_2) (\not{k}_2 - \not{k}_3) u, \\ iM_{F_2} &= -V_F \bar{v} (\not{k}_2 - \not{k}_3) G_A(p_1 - k_1) \not{k}_1 \gamma_5 u, \quad V_F = V_{p\bar{p}\eta} V_{p\bar{p}K \bar{K}}. \end{aligned} \quad (16)$$

Here, $m_{K\bar{K}}$ is the effective mass of $K\bar{K}$ system; $G_a = (4m^2 - m_a^2)^{-1}$ is the meson propagator ($a = \eta, \pi^0$), and m_a is the meson mass. The amplitudes $M_B(i, a)$ (14) are specified by the Lagrangian L_i ($i = 1, 2$), determining the 4-meson vertex of the diagram (B) in Fig. 2, and by the exchanged meson $a = \eta, \pi^0$. Representing the amplitudes in the form (9), we obtain

$$\begin{aligned} (A_{1,2,3}, D_{1,2}, F_{1,2}): \quad A, \mathbf{B} &= \text{(see Sections 2, 3 of Appendix);} \\ (B_{1,a}): \quad A &= -8V_{1a} m^2 (2m\omega_\eta + m_K^2 - m_{K\bar{K}}^2) G_a; \\ (B_{2,a}): \quad A &= -4V_{2a} m^2 G_a; \\ (C): \quad A &= 4V_C m^2 (2\omega_\eta - \omega_K - \omega_{\bar{K}}); \quad \mathbf{B} = 0 \text{ for } (B), (C); \end{aligned} \quad (17)$$

In the “threshold” approximation (11) we have $\mathbf{B} = 0$ and

$$\begin{aligned} (A_{1,2}): \quad A^{(0)} &= \frac{V_{p\bar{p}\eta} V_{p\bar{A}K}^2 2m\omega_\eta \omega_K^2}{(2m - m_\eta)(M_A + m - m_K)}; \quad (A_3): \quad A^{(0)} = \frac{V_{A\bar{A}\eta} V_{p\bar{A}K}^2 2m\omega_\eta \omega_K^2}{(M_A + m - m_K)^2}; \\ (B_{1,a}): \quad A^{(0)} &= -8V_{1a} m^2 (2m\omega_\eta - 3\omega_K^2) G_a; \quad (B_{2,a}): \quad A^{(0)} = \text{(see Eq. (17));} \\ (C): \quad A^{(0)} &= 8V_C m^2 (\omega_\eta - \omega_K); \quad (D_{1,2}): \quad A^{(0)} = V_D \frac{2m\omega_K (\omega_K - \omega_\eta)}{M_A + m - \omega_K}; \quad (F_{1,2}): \quad A^{(0)} = 0. \end{aligned} \quad (18)$$

3.3. A remark on power counting

Let us look at the tree approximation in connection with the ChPT power-counting rules and give the dimensional estimation of the amplitudes. We express the amplitudes through the following factors: V (the product of the vertex constants); $2m$ (normalization factor for bispinors, i.e. $\bar{u}u = 2m$); ω^n , where ω is typical value of the meson total energy (for the meson-baryon vertex of the diagrams (B) we replace $\omega \rightarrow 2m$) and n is the number of derivatives in the Lagrangian, determining a given vertex); $1/\omega$ and $1/4m^2$ for baryon and meson propagators, respectively. Let us rewrite the factors V through the dimensionless constants \bar{V} . Then, $V = \bar{V}m_\eta^2/f^3 \sim \bar{V}\omega^2/f^3$ for diagrams ($B_{2,a}$) in Fig. 2 (and diagram (B) in Fig. 1), and $V = \bar{V}/f^3$ for all the rest of diagrams. The resulting estimations of the diagrams in Figs. 1 and 2 are

$$(A) \sim (C) \sim (D) \sim (F) \sim \frac{\bar{V}}{f^3} 2m\omega, \quad (B) \sim \frac{\bar{V}}{f^3} \omega^2. \quad (19)$$

Since $\omega \sim 2m/3 \sim m$, the amplitudes (19) are approximately of the same order of magnitude. However, the \bar{V} values, fixed by the $SU(3)$ Lagrangian, are very different (these numbers are presented in Section 4 for the case of $K^+K^-\eta$ channel). Thus, the contributions of the tree diagrams are very different, especially in the $\bar{p}p \rightarrow \eta K^+K^-$ case, as discussed below.

4 The results

Applying the amplitudes of Section 3, defined by Eq. (9), we get the $p\bar{p}$ -annihilation cross section $v\sigma$ at rest ($v \rightarrow 0$) in the form

$$v\sigma(p\bar{p} \rightarrow \dots) = \frac{I}{4m^2} \int \overline{|M|^2} d\tau_3, \quad d\tau_3 = \frac{k_1 q \, dw dz}{32\pi^3 \sqrt{s}} \quad (\sqrt{s} = 2m). \quad (20)$$

Here, I is the identity factor, and $I = 1/3!$ ($I = 1$) for the $\eta\eta\eta$ ($\eta K\bar{K}$) channel; $\overline{|M|^2} = \frac{1}{2}(|A|^2 + |\mathbf{B}|^2)$ is the amplitude (9), squared and averaged over the initial p and \bar{p} spin states; $d\tau_3$ is the phase-space element (in the Feynman normalization) of the final 3-meson state, written for the unpolarized case; $k_1 = Q(\sqrt{s}, \mu_1, w)$ and $q = Q(w, \mu_2, \mu_3)$, where $Q(m, x, y)$ is the relative 3-momentum in the pair of particles with masses x and y , and m is the effective mass of this pair; w is the effective mass of the final meson pair (2+3), and $z = \cos \theta$, where θ is the polar angle of the relative motion in the (2+3) pair. The results obtained from Eqs. (20) with the amplitudes, given by Eqs. (10) or (17), will be referred to as the “exact” results.

We also give simplified (“threshold”) version of calculations, making use of the amplitudes, given by Eqs. (12) and (18). Then, the cross section can be written as

$$v\sigma^{(0)}(p\bar{p} \rightarrow \dots) = \frac{I}{8m^2} |A^{(0)}|^2 \tau_3^{(0)}, \quad \tau_3^{(0)} = \frac{(\mu_1 \mu_2 \mu_3)^{1/2} T^2}{64\pi^2 (\mu_1 + \mu_2 + \mu_3)^{3/2}}, \quad (21)$$

where $A^{(0)}$ is the sum of terms, given by Eqs. (12) or (18) for $\eta\eta\eta$ or $\eta K\bar{K}$ channels, respectively; $\tau_3^{(0)}$ is the nonrelativistic phase space [15] of final 3-meson state, and $T = 2m - \mu_1 - \mu_2 - \mu_3$ is the released energy.

Further we give the results in terms of branchings (Br), where

$$\text{Br}(p\bar{p} \rightarrow \dots) = \frac{v\sigma(p\bar{p} \rightarrow \dots)}{v\sigma_{p\bar{p}}^{\text{ann}}}, \quad v\sigma_{p\bar{p}}^{\text{ann}}(v \rightarrow 0) = 36.5 \text{ mb.} \quad (22)$$

The total $p\bar{p}$ -annihilation cross section $v\sigma_{p\bar{p}}^{\text{ann}}$ can be obtained from the imaginary part of s -wave scattering length $\text{Im}a_s = -0.69 \text{ fm}$, extracted in [16]. Then, we get $v\sigma_{p\bar{p}}^{\text{ann}}(v \rightarrow 0) = (8\pi/m) \text{Im}(-a_s) =$ the value in Eqs. (22).

Our numerical values of branchings as well as the experimental ones are presented in Table 1. We give both “exact” and “threshold” results (the latter are in brackets) for two sets – (a) [17] and (b) [18] – of values of D and F constants, which enter the term L_4 of the Lagrangian (6) and were determined from semileptonic baryon decays. These sets are

$$\begin{aligned} (a) \quad & D = 0.76, \quad F = 0.48 \text{ [17];} \\ (b) \quad & D = 0.80, \quad F = 0.46 \text{ [18].} \end{aligned} \quad (23)$$

The results in Table 1 show some sensitivity to D and F values. Let us consider different channels separately.

Table 1. The branchings for $p\bar{p}$ -annihilation reactions at rest (the data [13] were obtained in liquid H_2 target; the data set for 3η channel was extracted from $p\bar{p} \rightarrow 6\gamma$ and $p\bar{p} \rightarrow 10\gamma$ events; the $K^0\bar{K}^0\eta$ branching is obtained from $K_S K_S \eta$ data [13] as $\text{Br}(K^0\bar{K}^0\eta) = 2 \text{ Br}(K_S K_S \eta)$)

Channel	Br(theor) $\times 10^4$	Br(exp) $\times 10^4$ [13]
$\bar{p}p \rightarrow \eta\eta\eta$	(a) 0.424 (0.343) (b) 0.314 (0.275)	4.22 ± 0.24 (6γ) 3.93 ± 0.68 (10γ)
$\bar{p}p \rightarrow \eta K^0 \bar{K}^0$	(a) 1.488 (0.763) (b) 1.676 (0.510)	$2 \times (2.2 \pm 0.7)$
$\bar{p}p \rightarrow \eta K^+ K^-$	(a) 182. (0.0035) (b) 157. (0.0011)	—

$\bar{p}p \rightarrow \eta\eta\eta$. The calculated branchings underestimate the data [13] approximately by one order of magnitude. Let us consider our result (a) in more detail. The “exact” version of branching value exceeds the “threshold” one by $\sim 24\%$. The diagrams (A) and (B) of Fig. 1, taken separately, give the “exact” (“threshold”) $\text{Br}(\eta\eta\eta)$ values 4.65×10^{-8} (1.16×10^{-6}) and 4.50×10^{-5} (4.81×10^{-5}), respectively. Thus, the diagram (B) dominates and the interference of the diagrams (A) and (B) is destructive. The double-baryon-exchange diagram (A) gives very different and relatively small contributions in

the “exact”/“threshold” versions. The amplitude M_B is approximately the same in both versions.⁵⁾

$\bar{p}p \rightarrow \eta K^0 \bar{K}^0$. Our results (a), (b) underestimate data by a factor ~ 3 . The experimental branching should also include the channels with direct resonance production. One of them is the $\phi\eta$ channel, studied in the reaction $\bar{p}p \rightarrow \eta K^+ K^-$, and the extracted branching $\text{Br}({}^3S_1, \bar{p}\bar{p} \rightarrow \phi\eta \rightarrow K^+ K^- \eta) = (0.76 \pm 0.31) \times 10^{-4}$ [19–21], which should be the same in the $K^0 \bar{K}^0 \eta$ channel. Subtracting this value with weight factor $\frac{3}{4}$, we obtain $(2 \times 2.2 - \frac{3}{4} \times 0.76) \times 10^{-4}$, what is closer to our results. Some contribution should also come from the $f_0(1500)\eta$ channel [22] due to the decay $f_0(1500) \rightarrow K \bar{K}$ [23]. With these reservations we may accept the approach based on the diagrams of Fig. 2 as the “background” model for the $\bar{p}p \rightarrow \eta K^0 \bar{K}^0$ reaction at rest.

Contributions of the diagrams in Fig. 2 to the branching as well as signs of the cross terms are very different. The largest contributions come from the diagrams (B_{1,π^0}), ($D_{1+} + D_2$) and ($F_{1+} + F_2$), and corresponding $\text{Br}(K^0 \bar{K}^0 \eta) \times 10^4$ values for variant (a) are 2.30 (0.39), 3.09 (0.016) and 2.45 (0), respectively. The results of “exact” and “threshold” versions are drastically different, and the ($F_{1,2}$) terms vanish in the latter case.

$\bar{p}p \rightarrow \eta K^+ K^-$. For this reaction the calculated branching exceeds the result for $\text{Br}(K^0 \bar{K}^0 \eta)$ approximately by two orders of magnitude. The experimental value for the charged channel case is unknown. We roughly estimated it from the data on the annihilation frequency Y [20]. For the s -wave branching we may write $Y > (1 - f_p) \cdot \text{Br}(K^+ K^- \eta)$, where $\text{Br}(K^+ K^- \eta) = \frac{1}{4}\text{Br}({}^1S_0) + \frac{3}{4}\text{Br}({}^3S_1)$, and f_p is the fraction of annihilation from the p -wave states.⁶⁾ Taking the values $Y = (8.17 \pm 0.37) \times 10^{-4}$ [20] and $f_p = 0.13$ [19] for $\bar{p}p \rightarrow \eta K^+ K^-$ at rest in the liquid target, we obtain an estimation $\text{Br}(K^+ K^- \eta) < 9.4 \times 10^{-4}$ for the upper value. Thus, the theoretical value exceeds the estimated data by more than one order of magnitude.

It is worth noting that the “exact” version of our results exceeds the “threshold” one approximately by five orders of magnitude, i.e., the latter approximation does not work at all. Very small $\text{Br}(K^+ K^- \eta)$ values in the “threshold” version are due to cancellation of different terms in the total amplitude. Table 2 contains the branching values, obtained from different diagrams of Fig. 2 separately. Here, we give the “exact” and “threshold” results (the latter are in brackets) for variant (a) and absolute values $|\bar{V}|$ of coupling factors \bar{V} (see Eq. (19)) for each diagram. The subscripts Σ^0 and Λ specifies the exchanged baryon A in Fig. 2. Further, we discuss the results of the “exact” version.

The largest contributions come from the diagrams ($A_{1+2,\Lambda}$), ($A_{3,\Lambda}$), ($D_{1+2,\Lambda}$) and (F_{1+2}). Note that the terms ($D_{1+2,\Lambda}$) have the largest factor $|\bar{V}| = .238$ due to the large coupling constants, containing Λ baryon. With these terms excluded, i.e. for the incomplete set (A_{1+2+3,Σ^0}) + (B) + (C) + (D_{1+2,Σ^0}) of diagrams, we have $\text{Br}(K^+ K^- \eta) \times 10^4 = 6.2$. Successive addition of the terms (F_{1+2}), ($A_{1+2+3,\Lambda}$) and ($D_{1+2,\Lambda}$) give the values $\text{Br}(K^+ K^- \eta) \times$

⁵⁾The difference of $\text{Br}(\eta\eta\eta)$ values from diagram (B) comes from the phase space difference $\tau_3/\tau_3^{(0)} = 4.50/4.81$, where $\tau_3^{(0)}$ is the non-relativistic phase space in Eqs. (21).

⁶⁾Here, we neglect the correction factors $E({}^1S_0)$ and $E({}^3S_1)$ for the statistical weights $\frac{1}{4}$ and $\frac{3}{4}$ of 1S_0 and 3S_1 states, equating them to 1. For example, $E({}^3S_1) = 0.989$ for the liquid H_2 target [19].

$10^4 = 12.1, 42$ and 182 , respectively. Note that the cross terms from these contributions are constructive. Thus, we obtain a large branching value $\text{Br}(K^+K^-\eta) \gg \text{Br}(K^0\bar{K}^0\eta)$, and the main reason comes from the diagrams containing Λ exchange, which are absent in the neutral $K^0\bar{K}^0\eta$ channel.

Table 2. The branchings for $\bar{p}p \rightarrow \eta K^+K^-$ at rest from the diagrams of Fig. 2 (the subscripts Σ^0 and Λ specifies the exchanged baryon A)

Diagram	$\text{Br} \times 10^4$	$ \bar{V} $	Diagram	$\text{Br} \times 10^4$	$ \bar{V} $
(A_{1+2, Σ^0})	0.0092 (0.0029)	0.0038	(A_{3, Σ^0})	0.0095 (0.0023)	0.0086
$(A_{1+2, \Lambda})$	4.57 (1.35)	0.079	$(A_{3, \Lambda})$	5.52 (1.19)	0.177
$(B_{1, \eta})$	0.91 (0.16)	0.049	(B_{1, π^0})	2.55 (0.46)	0.089
$(B_{2, \eta})$	0.44 (0.46)	0.037	(B_{2, π^0})	0.14 (0.14)	0.045
(C)	0.44 (0.15)	0.069	(D_{1+2, Σ^0})	0.83 (0.0047)	0.030
$(D_{1+2, \Lambda})$	61.9 (0.32)	0.238	(F_{1+2})	10.6 (0)	0.098

5 Conclusion

The $p\bar{p}$ -annihilation processes $\bar{p}p \rightarrow \eta\eta\eta$ and $\bar{p}p \rightarrow \eta K\bar{K}$ at rest were considered in the tree approximation in the framework of the $SU(3)$ chiral effective Lagrangian at leading order. The following results were obtained.

1) The calculated branchings for the $\eta\eta\eta$ and $K^0\bar{K}^0\eta$ channels are several times smaller than the experimental values. Our results underestimate the data approximately by one order of magnitude in the $\eta\eta\eta$ case and – by ~ 3 times in the $K^0\bar{K}^0\eta$ one. One of the important missing contributions may be the direct production of intermediate heavy resonances, not incorporated into the pseudoscalar $SU(3)$ octet of mesons. Thus, for example, an essential role of the resonance $f_0(1500)$ in the $\eta\eta$ -mass spectrum was found in the reaction $\bar{p}p \rightarrow \eta\eta\eta$ at beam momenta 600-2410 MeV/c [22]. Due to a large $f_0(1500)$ width $\Gamma \approx 109$ MeV [23], one may also expect this resonance to affect visibly the calculated cross section of the reaction at rest. The other intermediate heavy resonances can also contribute. On the other hand, we can not exclude a sizeable role of the next-to-leading-order (NLO) corrections, including the loop diagrams. Potential $p\bar{p}$ -interaction in the initial state can also change the reaction cross sections calculated in the ChPT approximation [see, for example, [24]].

Thus, we consider our estimation of the tree diagrams as the calculation in the Born approximation and as the background model of the given processes.

2) The calculated branching for the $K^+K^-\eta$ channel exceeds the estimated data by more than one order of magnitude. Formally, the data on this branching are unknown, and our statement is based on rough estimation of the "experimental" value, given in Section 4. Perhaps, the possible resonance-production mechanisms as well as the NLO corrections could partly explain this strong discrepancy. However, here the results obtained seem to

be against the applicability of the chiral effective approach to the annihilation processes. An important reason of large calculated $K^+K^-\eta$ branching comes from the large $SU(3)$ vertex constants, involving Λ -baryon exchange (not occurring in the neutral $K^0\bar{K}^0\eta$ case). Perhaps, the NLO corrections may be also enhanced due the Λ vertices and improve the theoretical branching value. This is an opened question, faced to the further investigations.

Acknowledgements

The authors are thankful to C. Hanhart and V.G. Ksenzov for useful discussions. A.E.K. thanks grant NSh-4172.2010.2 for partial financial support.

Appendix

1. The terms of the Lagrangians L_{1-4} (6) for a given baryons (B) and mesons (π)

1.1. The four-meson terms of L_1 (6):

$$\begin{aligned}
L_1(\eta\eta K\bar{K}) &= V_{\eta\eta K\bar{K}}^{(1)}[\eta\partial_\mu\eta(K\partial^\mu\bar{K} + \bar{K}\partial^\mu K) - \partial_\mu\eta\partial^\mu\eta K\bar{K} - \eta\eta\partial_\mu K\partial^\mu\bar{K}], \\
L_1(\pi^0\eta K\bar{K}) &= V_{\pi^0\eta K\bar{K}}^{(1)}[(\pi^0\partial_\mu\eta + \eta\partial_\mu\pi^0)(K\partial^\mu\bar{K} + \bar{K}\partial^\mu K) - \\
&\quad - 2\partial_\mu\eta\partial^\mu\pi^0 K\bar{K} - 2\eta\pi^0\partial_\mu K\partial^\mu\bar{K}], \\
V_{\eta\eta K\bar{K}}^{(1)} &= \frac{1}{4f^2}, \quad V_{\pi^0\eta K^+K^-}^{(1)} = -V_{\pi^0\eta K^0\bar{K}^0}^{(1)} = \frac{1}{4\sqrt{3}f^2}.
\end{aligned} \tag{A.1}$$

1.2. The four-meson terms of L_2 (6):

$$\begin{aligned}
L_2(\pi_a\pi_b\pi_c\pi_d) &= \frac{1}{n!} V_{\pi_a\pi_b\pi_c\pi_d}^{(2)}\pi_a\pi_b\pi_c\pi_d, \\
V_{\eta^4}^{(2)} &= 4!\frac{m_\eta^2}{18f^2}, \quad V_{\eta\eta K\bar{K}}^{(2)} = 2!\frac{3m_\eta^2}{16f^2}, \quad V_{\pi^0\eta K^+K^-}^{(2)} = -V_{\pi^0\eta K^0\bar{K}^0}^{(2)} = -\frac{m_\eta^2}{8\sqrt{3}f^2}.
\end{aligned} \tag{A.2}$$

Here, we introduce the identity factor $n!$, where $n = 4(\eta^4)$, $2(\eta\eta K\bar{K})$, $1(\pi^0\eta K\bar{K})$.

1.3. The terms of L_3 (6) for $B_a\bar{B}_b \rightarrow \pi_c\pi_d$:

$$\begin{aligned}
L_3(B_a\bar{B}_b\pi_c\pi_d) &= iV_{B_a\bar{B}_b\pi_c\pi_d}\bar{u}_b\gamma_\mu u_a(\pi_d\partial^\mu\pi_c - \pi_c\partial^\mu\pi_d), \\
V_{p\bar{\Sigma}^+K^0\eta} &= -V_{\Sigma^+\bar{p}K^0\eta} = \frac{\sqrt{3}}{4\sqrt{2}f^2}, \quad V_{p\bar{\Lambda}K^+\eta} = -V_{\Lambda\bar{p}K^-\eta} = \frac{3}{8f^2}, \\
V_{p\bar{\Sigma}^0K^+\eta} &= -V_{\Sigma^0\bar{p}K^-\eta} = \frac{\sqrt{3}}{8f^2}, \quad V_{p\bar{p}K^+K^-} = \frac{1}{2f^2}, \quad V_{p\bar{p}K^0\bar{K}^0} = \frac{1}{4f^2};
\end{aligned} \tag{A.3}$$

1.4. The terms of L_4 (6) for $B_a\bar{B}_b \rightarrow \pi_c$:

$$L_4(B_a\bar{B}_b\pi_c) = V_{B_a\bar{B}_b\pi_c}\bar{u}_b\gamma_\mu\gamma_5 u_a\partial^\mu\pi_c, \quad V_{B_a\bar{B}_b\pi_c} = V_{B_b\bar{B}_a\pi_c};$$

$$\begin{aligned}
V_{p\bar{p}\eta} &= \frac{3F - D}{2\sqrt{3}f}, & V_{p\bar{p}\pi^0} &= \frac{D + F}{2f}, & V_{p\bar{\Sigma}^0 K^+} &= \frac{D - F}{2f}, \\
V_{p\bar{\Sigma}^+ K^0} &= \frac{D - F}{\sqrt{2}f}, & V_{p\bar{\Lambda} K^+} &= -\frac{D + 3F}{2\sqrt{3}f}, & V_{\Sigma\bar{\Sigma}\eta} &= -V_{\Lambda\bar{\Lambda}\eta} = \frac{D}{\sqrt{3}f};
\end{aligned} \tag{A.4}$$

1.5. The terms of L_4 (6) for $p\bar{p} \rightarrow \eta K \bar{K}$:

$$\begin{aligned}
L_4(p\bar{p}\eta K \bar{K}) &= V_{p\bar{p}\eta K \bar{K}} \bar{u}_{\bar{p}} \gamma_\mu \gamma_5 u_p [2K \bar{K} \partial^\mu \eta - \eta(\bar{K} \partial^\mu K + K \partial^\mu \bar{K})], \\
V_{p\bar{p}\eta K^0 \bar{K}^0} &= \frac{D - F}{8\sqrt{3}f^3}, & V_{p\bar{p}\eta K^+ \bar{K}^-} &= \frac{-F}{4\sqrt{3}f^3};
\end{aligned} \tag{A.5}$$

$u_p(\bar{u}_{\bar{p}})$ is the Dirac spinor of the proton (antiproton) in items 1.3-1.5.

2. The amplitudes M_A and $M_{A_{1,2,3}}$

For the amplitude M_{A_1} , represented in the form (9), we obtain

$$(A_1): \quad A = c[a + b(\mathbf{k}_1 \mathbf{k}_3)], \quad \mathbf{B} = cb[\mathbf{k}_3 \times \mathbf{k}_1], \tag{A.6}$$

where

$$\begin{aligned}
c &= 2mV D_1^{-1} D_3^{-1}, \quad D_{1,3} = m^2 - 2m\omega_{1,3} + \mu_{1,3}^2 - M_{1,3}^2, \\
a &= B_3(A_1 k_1^2 + B_1 \omega_2) + B_1 A_3 k_3^2, \quad b = A_1(B_3 + A_3 \omega_2) + B_1 A_3, \\
A_{1,3} &= m + M_{1,3}, \quad B_{1,3} = (M_{1,3} - m)\omega_{1,3} + \mu_{1,3}^2.
\end{aligned}$$

Here: $V = V_{p\bar{p}\eta} V_{pAK}^2$ is the vertex production; \mathbf{k}_i , ω_i and μ_i are, respectively, the 3-momentum ($k_i = |\mathbf{k}_i|$), total energy and mass of the final meson (see Fig. 2); $M_{1,3}$ are the exchanged-baryon masses ($M_1 = m$ and $M_3 = m_A$ for the diagram A_1 in Fig. 2). The amplitudes M_A (Fig. 1) and the rest of the amplitudes M_{A_i} (Fig. 2) can be obtained from Eq. (A.6) by the proper replacement of the vertex factor V , final-meson momenta and baryon masses M_i .

3. The amplitudes $M_{D_{1,2}}$ and $M_{F_{1,2}}$

For these amplitudes, represented in the form (9), we obtain

$$\begin{aligned}
(D_{1,2}): \quad A &= c_{1,2}[a_{1,2} + b(k_1^2 - k_3^2)], & \mathbf{B} &= 2c_{1,2} b[\mathbf{k}_3 \times \mathbf{k}_2]; \\
(F_{1,2}): \quad A &= c[(\omega_{3,2} - \omega_{2,3})\mu_1^2 + 2m(k_{3,2}^2 - k_{2,1}^2)], & \mathbf{B} &= 4cm[\mathbf{k}_{1,3} \times \mathbf{k}_{2,1}].
\end{aligned} \tag{A.7}$$

Here,

$$\begin{aligned}
c_{1,2} &= -2mV_D D_{1,2}^{-1}, \quad D_{1,2} = m^2 - 2m\omega_{3,2} + \mu_{3,2}^2 - m_A, \\
a_{1,2} &= (\omega_1 - \omega_{2,3})[(m_A - m)\omega_{3,2} + \mu_{3,2}^2], \quad b = m + m_A, \\
c &= -2mV_F(\mu_1^2 - 2m\omega_1)^{-1};
\end{aligned}$$

V_D and V_F are the vertex productions (16).

References

- [1] S. Weinberg, *Physica A* **96**, 327 (1979).
- [2] J. Gasser and H. Leutwyler, *Ann. Phys.* **158**, 142 (1984).
- [3] G. Colangelo, J. Gasser, and H. Leutwyler, *Nucl. Phys. B* **603**, 125 (2001); hep-ph/0103088.
- [4] J. Gasser, M. E. Sainio, and A. Svarc, *Nucl. Phys. B* **307**, 779 (1988).
- [5] N. Fettes and U.-G. Meißner, *Nucl. Phys. A* **693**, 693 (2001); hep-ph/0101030.
- [6] S.R.Beane, P.F. Bedaque, W.C.Haxton, *et al.*, *At the Frontier of Particle Physics* (World Sci. Singapore, 2001), Vol. 1, p. 133; nucl-th/0008064.
- [7] E. Epelbaum, *Prog. Part. Nucl. Phys.* **57**, 654 (2006); nucl-th/0509032.
- [8] V. Bernard, N. Kaiser, and Ulf-G. Meißner, *Int. J. Mod. Phys. E* **4**,193 (1995); hep-ph/9501384.
- [9] A. Manohar, hep-ph/9606222.
- [10] S. Scherer, *Adv. Nucl. Phys.* **27**, 277 (2003); hep-ph/0210398.
- [11] R. Machleidt and D. R. Entem, *Phys. Rept.* **503**, 1 (2011); arXiv:1105.2919 [nucl-th].
- [12] E. Klempt, Ch. Batty, and J.-M. Richard, *Phys. Rept.* **413**, 197 (2005); hep-ex/0501020.
- [13] C. Amsler *et al.*, *Nucl. Phys. A* **720**, 357 (2003).
- [14] M. Gell-Mann, R. J. Oakes, and B. Renner, *Phys. Rev.* **175**, 2195 (1968).
- [15] I. S. Shapiro, *UFN* **92**, 549 (1967).
- [16] J. Carbonel, K. V. Protasov, and A. Zenoni, *Phys. Lett. B* **397**, 345 (1997); nucl-th/9806032.
- [17] L. B. Okun, *Leptons and Quarks* (Nauka, Moscow, 1990), Chapt. 6, p. 51.
- [18] B. Kubis, hep-ph/0703274.
- [19] The OBELIX Collab. (A. Alberico *et al.*), *Phys. Lett. B* **432**, 427 (1998).
- [20] The OBELIX Collab. (V. Nomokonov), *Acta Phys. Polon. B* **29**, 2547 (1998).
- [21] V. P. Nomokonov and M. G. Sapozhnikov, *Phys. Part. Nucl.* **34**, 94 (2003) [*Fiz. Elem. Chastits At. Yadra* **34**, 189 (2003)].

- [22] A. V. Anisovich *et al.*, arXiv:1109.4008 [hep-ex].
- [23] K. Nakamura *et al.* (Particle Data Group), J. Phys. G **37**, 075021 (2010)
(available at <http://pdg.lbl.gov>).
- [24] I. S. Shapiro, Phys. Rept. **35**, 129 (1978).

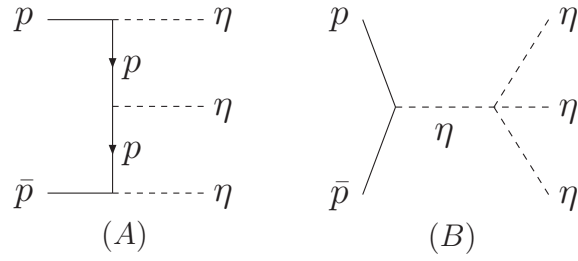


Figure 1: Feynman tree diagrams for the $\bar{p}p \rightarrow \eta\eta\eta$ amplitude. Solid and dashed lines correspond to the baryons and mesons, respectively.

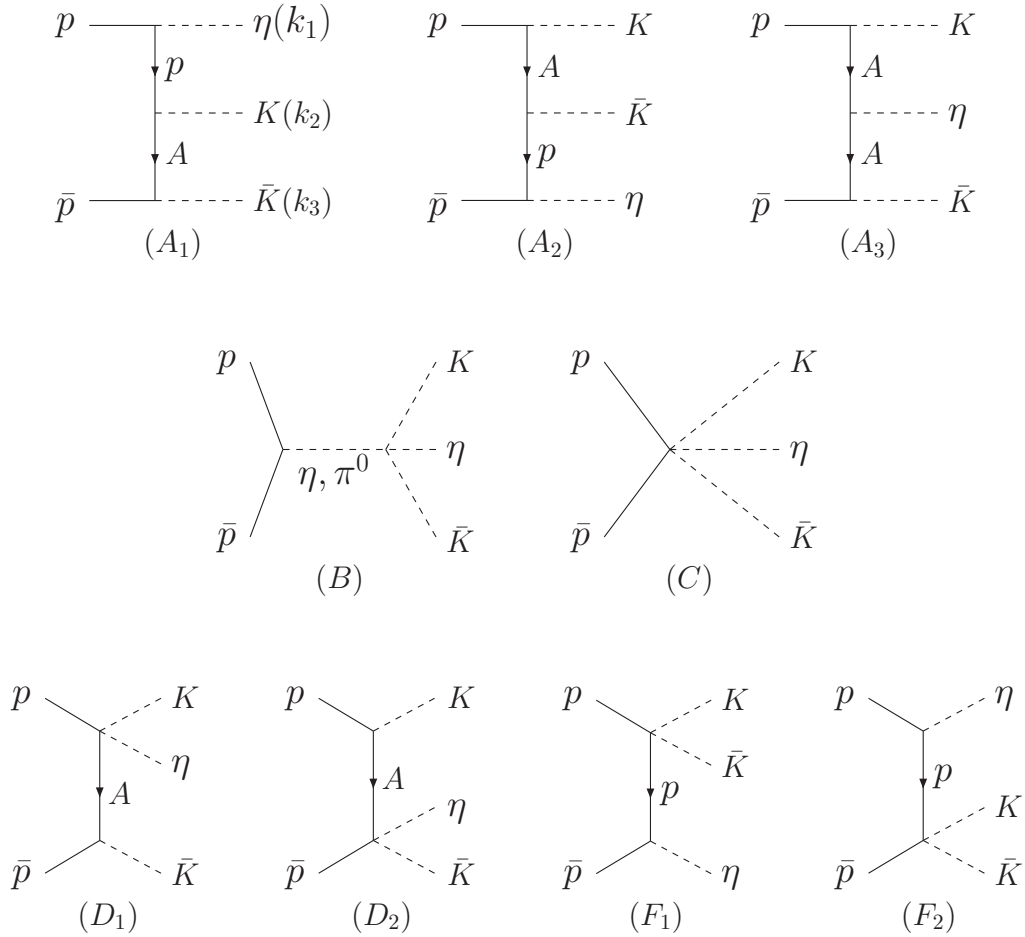


Figure 2: Feynman tree diagrams for the $\bar{p}p \rightarrow \eta K \bar{K}$ amplitude. Lines are the same as in Fig 1. The exchanged baryon A is Σ^+ (Σ^0 or Λ) in the case of the $\eta K^0 \bar{K}^0$ ($\eta K^+ K^-$) channel.